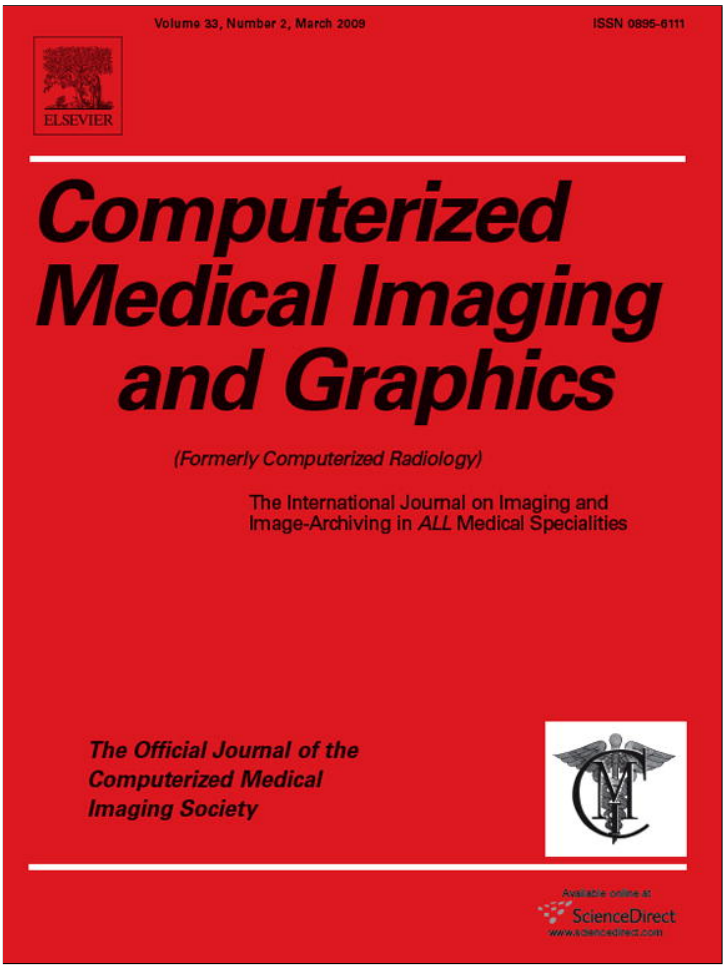

Computerized Medical Imaging and Graphics 33 (2009) 83–90

Contents lists available at ScienceDirect

Computerized Medical Imaging and Graphics

journal homepage: www.elsevier.com/locate/compmedimag

Practical application of contrast-enhanced magnetic resonance mammography [CE-MRM] by an algorithm combining morphological and enhancement patterns

Giuseppe Potente*, Daniela Messineo, Claudia Maggi, Sara Savelli

Department of Radiological Sciences, University of Rome "La Sapienza", Viale Regina Elena 324, 00161 Rome, Italy

ARTICLE INFO

Article history:
Received 28 November 2005
Received in revised form 22 March 2008
Accepted 10 October 2008

Keywords:
Breast lesion
Magnetic resonance imaging
Contrast enhancement
Problem solving
Wash out
Diagnostic algorithm

ABSTRACT

The purpose of this article is to report our practical utilization of dynamic contrast-enhanced magnetic resonance mammography [DCE-MRM] in the diagnosis of breast lesions. In many European centers, was preferred a high-temporal acquisition of both breasts simultaneously in a large FOV. We preferred to scan single breasts, with the aim to combine the analysis of the contrast intake and washout with the morphological evaluation of breast lesions. We followed an interpretation model, based upon a diagnostic algorithm, which combined contrast enhancement with morphological evaluation, in order to increase our confidence in diagnosis. DCE-MRM with our diagnostic algorithm has identified 179 malignant and 41 benign lesions; final outcome has identified 178 malignant and 42 benign lesions, 3 false positives and 2 false negatives.

Sensitivity of CE-MRM was 98.3%; specificity, 95.1%; positive predictive value, 98.9%; negative predictive value, 92.8% and accuracy, 97.7%.

1. Introduction

Breast cancer is the most frequency malignancy in women. X-rays mammography is still the most widely used imaging modality for early detection of clinically occult breast cancer. All over the world, mammography is used as a screening method for detection of breast cancer but its sensitivity is limited in some cases [1–3]. The gold standard in clinical practice is still currently association of mammography with ultrasound, physical examination and needle biopsy, that someone calls triple assessment [1].

Dynamic contrast-enhanced [DCE] magnetic resonance imaging mammography [MRM] is a valuable complementary modality to conventional diagnostic method. In the last years, nevertheless, despite its high sensitivity, breast MRI has played a limited role, mostly restricted to evaluation of high risk young women, follow-up of patients after radiotherapy, and evaluation of suspected lesions in silicon prosthesis.

When we began our research – in 1999 – there were many unresolved issues in breast MR imaging, including no definite standard technique for contrast-enhanced MRM [CE-MRM], no standard interpretation criteria for evaluating such studies, no consensus on what constitutes clinically important enhancement, and no clearly defined clinical indications for the use of MRM [5]. In many European centers, it was preferred a high-temporal-resolution acquisition of both breasts simultaneously in a large FOV [>300 mm × 300 mm] [4,5]. In many state-of-the-art centers, otherwise, it was preferred to analyze lesion architecture on high-spatial-resolution in single breasts, mostly in the sagittal plane. The preference for the sagittal plane was probably due to the relative ease of correlating a finding identified on a sagittal MR image with a finding on a mediolateral oblique or mediolateral mammographic view [4,5]. Imaging of single breasts increases the resolution, and improves the evaluation of morphology of lesions. The preference for morphological evaluation was based upon well supported studies that architectural features, identified on high-spatial-resolution images, can characterize lesions as likely malignant or likely benign, with a lesser overlap than enhancement characteristics of malignant and benign lesions [5].

To provide a consensus in lexicon and in evaluation, in 1998 a Lesion Diagnosis Working Group was formed in USA. A concurrent goal was to develop scan technique reporting recommendations, as well to suggest MRI techniques that would provide state-of-the-art images and kinetic data based on the best available information to date [7]. In their preliminary report, the authors pointed out the

* Corresponding author. Tel.: +39 06 44237288.
E-mail address: giuseppe.potente@uniroma1.it (G. Potente).

0895-6111/$ – see front matter © 2008 Elsevier Ltd. All rights reserved.
doi:10.1016/j.compmedimag.2008.10.004

great variability of MRI techniques in the world and the different criteria to determine whether lesions detected by breast MRI are benign or malignant:

1. Lesion architecture;
2. Time-course enhancement;
3. Novel technologies.

In order to monitor intensity value of the contrast agent uptake [washin] and subsequent decrease in intensity [washout], the region of interest [ROI] is imaged repeatedly, resulting in a signal–time function for each voxel within the entire tissue volume: analysis and interpretation of these signal–time curve can give, in the opinion of many authors [1,24–28] an useful information on both the location and type of lesion.

In interpreting the signal–time curves resulting from DCE-MRI volumes, it is possible evaluate both the early [before 2 min] slope and the delayed [after 2 min] slope of the curve. A number of quantitative and estimation techniques have been proposed by the researchers to interpret the signal–time curves in the early phase [*washin*], including the time delay between vessel enhancement and lesion enhancement [9]. In estimating the delayed phase of the curve, a three-category classification is currently in use [1]. Curves are classified as type I: steady enhancement; type II: plateau of signal intensity; type III: *washout* of signal intensity. Kuhl et al. found a global accuracy of signal intensity time data in differential diagnosis of enhancing lesions [25].

Some authors, e.g. Subramanian et al. [1] think that kinetic curves have some disadvantages.

One disadvantage is the high-temporal resolution that is needed for maintaining accuracy, which in turn limits the size of the region being imaged. Overall accuracies of these techniques have a considerable variance in terms of lesion sensitivity and specificity, and thus have not gained a wide acceptance to date [1]. When there are multiple cancerous volumes, analyzing signal–time curves becomes tedious and error-prone, and requires examining individual voxels in image slices, depending on the tools available at a site [1]. We agree with these opinions.

In our work, we therefore decided to obtain the best compromise [by our machine] between high-temporal resolution and high-spatial resolution, to combine analysis of the contrast intake and washout with morphological evaluation of breast lesions, without obtaining kinetic curves. Our aim was to design an MRI diagnostic algorithm for a two-class problem in a way that the algorithm is developed on a training set of data [on samples where the histological diagnosis is known], and then evaluated on a following validation [test] phase in the reported present set, for which we report a classification performance such as its "sensitivity" and "specificity". Our aim was also to reduce the time consumed in examinations and consequently the cost of MRM.

A similar algorithm was described in a paper by other authors [6], published after the beginning of our research. Several studies have shown that DCE-MRM has a higher sensitivity than mammography in detection and diagnosis of invasive breast cancer [10]. In contrast, the literature reports varying results concerning specificity [1,3]. The association of both architectural and kinetic information extracted [12], from dynamic CE-MRI can improve diagnostic performance [6,27].

In our prospective study we have evaluated both the features of mass lesions and the value of different established diagnostic criteria of breast DCE-MRM that contributed to the diagnostic performance.

2. Materials and methods

2.1. Patients

Before this prospective work, we performed a trial research on 100 patients in 1999–2000. This preliminary training study was accomplished by two of us (G.P., a reader, and C.M., the resident in charge of research protocol).

In the present paper, we report a prospective examination of 210 consecutive patients, all females, aged between 25 and 80 years of age (mean, 56.6 years) from January 2001 to July 2003; there were 144 postmenopausal women. In this update work, the readers were G.P. and D.M.; the residents in charge of the protocol were C.M. and S.S.

The reasons for referral were numerous: discrepancies in the results using other methods, preoperative assessment for breast cancer, discovery of some palpable axillary masses, follow-up after conservative surgery for breast cancer. In our study were found 220 mammary lesions. Most (87%) of the 220 MRI abnormal findings were corresponding to palpable or mammographic lesions.

2.2. MR imaging protocol

All the patients were examined using a Siemens 1.5 Tesla system (Magnetom Vision Plus) set up at the Department of Radiological Sciences of "Sapienza" University of Rome. The time of the menstrual cycle was registered, and the examination was deferred if it was preferable, due to the possible enhancement of normal breast tissue.

Patients were examined in the prone position with breasts suspended in a double breast coil at the isocenter of the magnet. To reduce movement artifacts, the possible gap between the inner wall of the coil and the breasts was packed with cotton batting. A transverse localizing image is acquired, followed by a sagittal T2 weighted sequences (TR/TE: 9128/60; FA: 180°; matrix 242×256; slice thickness Th: 3 mm; intersection gap: 1 mm; FOV: $105–200 \times 200$ mm) for each breast. Non-enhanced and enhanced three-dimensional (3D) fast low-angle shot (FLASH) T1 sequences in the sagittal plane (TR/TE: 12–15/5; slice thickness: 1.5–3 mm; acquisition matrix: $112–252 \times 256$; flip angle: 20°), covering the entire breast. The field of view was adjusted to fit breast size, ranging from 105 to 200 mm. The number of slices ranged from 34 to 53, depending on individual breast size. Acquisition times ranged between 87 and 110 s (Table 5) depending on the number of slices. Suppression of the fat signal was attained in a "passive" way, with post-processing image subtractions.

For dynamic contrast enhancement, gadopentate dimeglumine in a weight-related dose (0.1 mmol/Kg) was injected in a bolus pattern for a duration of 15 s, followed by saline infusion in bolus administered by automatic injector. Contrast-enhanced images were obtained starting at least 20 s after the end of the bolus

Post-contrast T1-weighted FLASH 3D images were obtained for each breast within the first 2 min after the bolus, at two different times, depending on the size of the breasts and consequently upon the time expended for the acquisition: with the longest time (110 s) necessary for the largest breasts, 20 and 420 s after the end of the bolus, for the first breast; 130 and 530 s after the end of the bolus for the second breast, in two interposed and following sequences. With the shortest time (87 s): for the first breast 20 and 420 s after the end of the bolus; for the second breast, 107 and 507 s after the end of the bolus.

We scan first the breast of interest, i.e. with palpable or mammographic lesions. In this way, the wash-in and wash-out phases of any pathological formations could be detected in both breasts, by the FLASH 3D sequences.

Kinetic signal–time curves were not used in this study: it is not possible to get reliable curves with only the pre-contrast and an early and a late phase.

In the present study, spatial resolutions [voxels] from 1.9 to 2.1 mm^3 were obtained, while the signal-to-noise ratios [SNR] was under 1.0. The loss of SNR was evaluated in a pilot group of 20 patients and was considered acceptable, before to begin the protocol.

2.2.1. Subtraction algorithm

1. The pre-contrast T1 FLASH 3D images was subtracted from the corresponding post-contrast early and late images on a pixel-by-pixel basis by using the software subtraction function available on the Siemens console, to screen for enhancing lesions.
2. A step-by-step subtraction algorithm (each dynamic phase image minus one-step prior phase image) to show the enhancing pattern between temporal phases.
3. A reverse subtraction algorithm (the last phase image was subtracted from each dynamic phase image), to aid the detection of early enhancing (wash-in) and wash-out.

The average post-processing time except image acquisition was approximately 10 min.

The same method was independently used by other authors [27].

2.2.2. MIP reconstruction

The maximum intensity pixel (MIP) technique was subsequently used to obtain 3D images of the breast examined which is essential for the purpose of locating the suspected pathological formation.

2.3. MR imaging analysis

In our clinical practice, MR imaging examinations were interpreted by two independent radiologists (readers: G.P., D.M.), in conjunction with clinical history and other breast imaging studies including mammograms, sonograms, and scintimammograms when available.

Areas of early (washin) or late enhancement in the breast in MIP images, whether or not the enhancement corresponded to the clinically or radiologically suspicious area, were considered to be abnormal (classes 2–4 in a scale reported below). The side (left or right breast), size, site and number of these areas were noted. In describing a focal mass or a focal enhancement we have followed the recommendations of Lesion Diagnosis Working Group [8].

2.3.1. Qualitative analysis

The *morphological parameters* analyzed were: shape and characteristics of margin (smooth, spiculated, irregular or lobulated borders). Irregular shape and irregular borders, scalloped and lobulated shape or borders were considered equivalent. For example, in Fig. 1 we have considered irregular shape and margin of the focal enhancements; otherwise, in Fig. 2 the focal enhancement was evaluated as smooth or regular.

The *dynamic parameters* investigated were presence or absence of enhancement within the first 2 min after the bolus (initial enhancement phase), the enhancement pattern (focal, linear, regional, ductal, patchy or diffuse), the enhancement pattern 7 min after the bolus and the internal architecture (enhancement pattern within a specific MRI distribution pattern). These aspects were *visually* evaluated.

2.3.2. Quantitative analysis

Measurements of enhancement has been included as a complementary method in the present study. Signal intensity measurements were performed only in selected cases, and excluded from the results in the Tables 1–5.

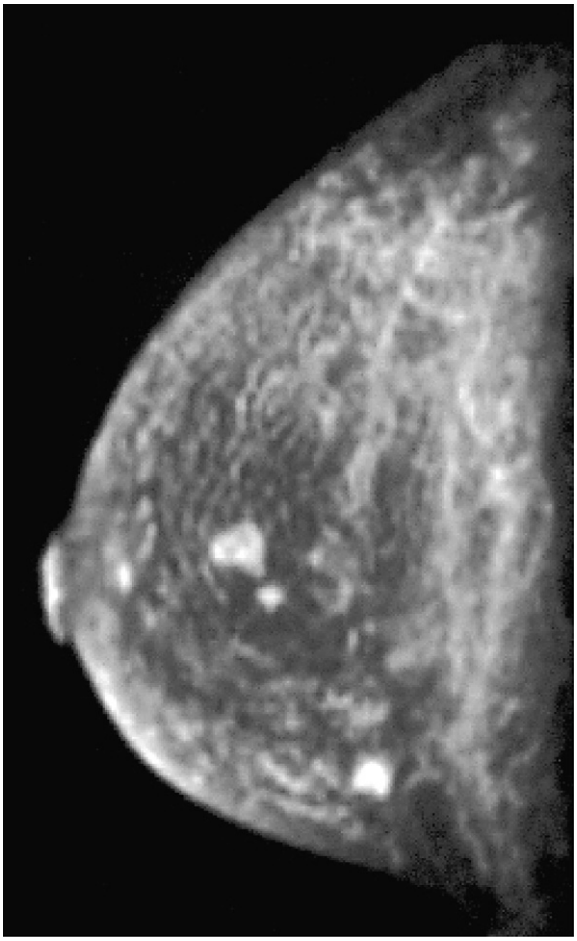

Fig. 1. Invasive ductal carcinoma in a 49-year-old woman. Not-palpable. (a) MIP of sagittal subtracted contrast-enhanced MR 3D FLASH T1 gradient-echo images shows three not-palpable 0.3–0.5 mm-irregular rim-enhancing formations, not demonstrated in previous imaging different modalities. A significant washout was visible in the late post-contrast scans (not shown).

Quantitative analysis was performed in all the lesions in the training preliminary study. Signal intensity measurements were performed in region of interest (ROIs) with focal enhancement of the breast during each dynamic phase. Signal intensities measured on post-contrast images were normalized by dividing the measurement by the pre-contrast signal intensity and then by multiplying by 100 to produce enhancement values. Signal intensity was measured in ROIs, with maximal enhancement in the lesion, as determined by means of visual inspection of the dynamic MR images. A ROI size of at least 3 pixel (area >2 mm^2) was utilized. The ROI with the maximum signal intensity increase within each lesion or tissue was selected for further analysis. Curves of normalized signal intensity over time were established from the measurements.

Evaluation based upon the quantitative analysis was coinciding with outcome based upon simple visual inspection of signal intensity, therefore we decided to utilize quantitative analysis only as complementary tool in validation research, to shorten the practical diagnostic procedure.

In our radiological practice, the MRM scans were interpreted by a breast subspecialist (G.P.) with knowledge of the clinical history and of the mammographic and ultrasound findings. The level of suspicious malignancy was classified in a scale of 0–4 classes. Class 0, assessment incomplete; Class 1, no abnormal enhancement

Table 1
The DCE-MRM parameters (columns) and the DCE-MRM evaluations vs. the final outcomes (rows) in 220 lesions.

MRI parameters	Benign ($n=41$) MRM diagnosis	True benign ($n=39$) final outcome	Malignant ($n=179$) MRM diagnosis	True malignant ($n=178$) final outcome
Margins				
Not evaluable	4	4	0	0
Smooth	10	10	5	5
Lobulated	5	6	5	4
Irregular	17	16	58	59
Spiculated	5	6	111	110
Degree of enhancement				
None	5	5	0	0
Low	4	4	0	0
Intermediate	21	20	27	28
Intense	11	11	152	152
Pattern of enhancement				
None	5	5	0	0
Progressive	26	26	16	16
Washout	5	5	152	152

(physiologic enhancement or no enhancement); Class 2, probably benign enhancement (fibroadenomas or other benign processes); Class 3, possibly benign lesion, to control after a short period within six months, if necessary in a different menstrual time (a malignant or borderline process cannot be ruled out); Class 4, suspicious or strongly suggestive of malignancy. The lesions in Class 0 have been excluded from this study.

2.3.3. Final outcome

The lesions comprised in the Classes 2, 3 and 4 underwent cytological or histological confirmations. In two cases in Class 2, the lesions were stable in the last two years and the radiological diagnosis of probable fibroadenomas was not confirmed neither by cytology or by histology.

An intra-observer analysis of the diagnostic evaluations was performed by comparing the two interpretative results from one radiologist (G.P.), at the time zero (January 2001) and after a period of 24 months (January 2003). Inter-observer variability was studied correlating the different results from two radiologists with different training in breast MRI evaluation (G.P. and D.M.). The variability was determined on the basis of non-weighted kappa statistics. We have considered: *slight* an agreement with kappa value from 0.0 to 0.2; *fair* a kappa value from 0.2 to 0.4; *moderate*, a kappa value from 0.4 to 0.6; *substantial* a kappa value from 0.6 to 0.8. A kappa value greater than 0.8 has been considered a *perfect* agreement.

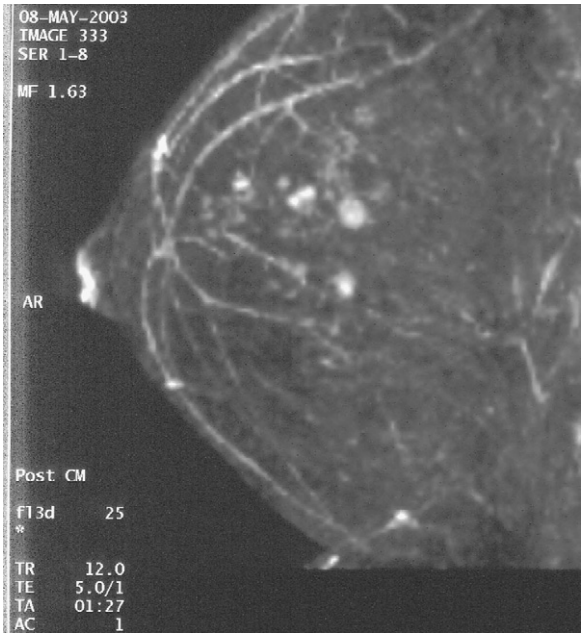

Fig. 2. Not-fibroadenomatous not-palpable benign small lesions in a 37-year-old woman. Maximum intensity pixel-by-pixel post-processing of subtracted FLASH 3D T1 gradient-echo MR sagittal images shows small enhancing smooth masses. An evident washout was absent in the delayed phase of DCE-MRM (not shown).

3. Results

The washout of the individual lesions was first searched for, obtaining 157 cases in which it was present and 63 cases in which it was absent. In the subsequent step, the borders of the lesions were examined. The lesions without washout and with smooth or regular borders have been defined lesions in Class 2. The formations that exhibited washout, with smooth borders, were classified in Class 3 (a malignant or borderline process cannot be ruled out). Twenty-seven pathological formations without washout, with spiculated borders, were considered as lesions in Class 4 (highly suspicious or strongly suggestive of malignancy).

Table 1 shows the frequency of the parameters used to determine the nature of the breast formations studied using MRI.

A total of 179 malignant (Class 4) and 41 benign (Classes 1–3) breast formations were assessed upon our diagnostic algorithm (Table 2). All the formations diagnosed as malignant ones displayed an intense ($n=152$) or an intermediate ($n=27$) enhancement; 152 (85%) of the 179 formations suspected of malignancy displayed a washout. The borders of the MRM-malignant lesions were more frequently spiculated ($n=111$) or irregular ($n=58$). Ten out of these 179 formations (5.3%) suspected of malignancy displayed smooth or lobulated borders.

In benign formations, all the morphological parameters set out in the Table 1 were found: the most frequently represented group showed irregular borders ($n=17$). The majority of the benign formations displayed an intermediate ($n=21$) or intense ($n=11$) level of enhancement. The benign formations showed in 26 cases a progressive pattern of enhancement.

All the MRM evaluations (except in two cases in Class 2) were compared with the final outcome (Table 3).

In 41 benign formations at the final outcome, 39 cases of true negatives and three cases of false positives were found. In 178 true malignant formations, 176 true positives and two false negatives were diagnosed.

Five benign formations with washout were found corresponding, on histological examination, to cystic fibroadenosis ($n=2$) or to fibroadenomas ($n=3$). Four of these lesions were correctly

Table 2
MRI diagnostic algorithm.

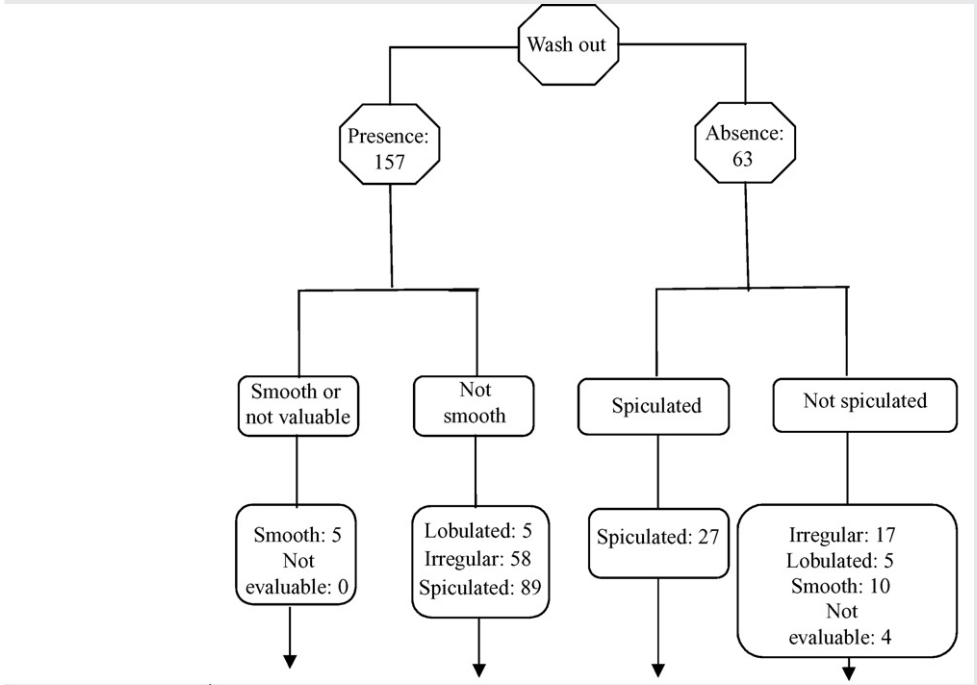

MRI diagnosis	Benign	Malignant	Malignant	Benign
	5	152	27	36
Classes	1-3	4	4	1-3
Final Outcome	4 True	150 True	26 True	35 True

diagnosed in Class 2 upon morphological parameters, one fibroadenoma with irregular margins was classified a lesion in Class 3 (a malignant process was not ruled out).

Sensitivity, specificity, positive predictive value, negative predictive value and diagnostic accuracy were calculated (sensitivity: 98.3%; specificity: 95.1%; positive predictive value: 98.9%; negative predictive value: 92.8; accuracy: 97.7%).

The results of intra-agreement and inter-agreement evaluations are presented in Table 4.

4. Discussion

DCE-MRM with dedicated breast coils is currently the most sensitive diagnostic procedure for detecting or excluding the presence of a pathological mammary pathology [6–9,11].

Table 3
Correlation between the MRI diagnosis of malignancy and the final outcome.

		Final outcome		Total
		Positive	Negative	
DCE	+	176	3	179
MRM	–	2	39	41
Total		178	42	220

Sensitivity: 98.3%; positive predictive value: 98.9; specificity: 95.1%; negative predictive value: 92.8; accuracy: 97.7%.

Despite its high sensitivity, in 5–10% of cases MRI is however unable to recognize whether the nature of the formation is benign or malignant because an increase of breast vascularization and of MRI enhancement could be caused either by the cyclic modifications to which the mammary gland undergoes before menopause, or by the presence of a mass [13,14]. Furthermore benign pathologies such as fibroadenomas occasionally show similar signal intensity to malignant tumors [4,14,15,19,26]. In many studies, anyway, DCE-MRM has proved to be the imaging method that most closely approaches the 'gold standard' represented by histopathological examination [5,16,17,20,22]. Therefore, is worthwhile any effort to improve the standardization of DCE-MRM, in order to gain its larger use in clinical management of breast cancer. Our purpose was to enhance the *practical* application of CE-MRM in breast pathology management.

In our work, we have examined breasts one by one to maximize the spatial resolution of the MRI. To reduce the discomfort of patients, we performed bilateral alternate scans in the same examination, without deferring the contrast dynamic MRM study. After that the present study was completed, a new machine (Siemens Avanto) with a developed software began to work in our Institution: this new equipment permits to plan an automated sagittal interleaved scanning of single breasts.

The knowledge of clinical and other imaging studies in MRM diagnosis has probably affected the accuracy of MRM diagnosis. Nevertheless, *ductal carcinoma in situ* (DCIS) may sometimes exhibit different behavior and compromise our correct diagnosis. Two DCIS in our group enhanced in the initial enhancement phase, without

Table 4
Intra and inter-observer variability assessed by Kappa factor in MRI analysis of the two groups of patients.

Features	Variability			
	Group I: no wash out ($n = 67$)		Group II: evidence of wash out ($n = 153$)	
	Intra	Inter	Intra	Inter
Spiculated borders	0.54	0.43	0.72	0.48
Enhancement degree and washin	0.63	0.52	0.81	0.71
Washout	0.54	0.42	0.97	0.82

showing an evident washout (Fig. 3). By the most currently used MRI sequences there is some degree of reduced confidence in DCIS diagnosis. Combination of mammography and MRM can improve the global accuracy in global management of these lesions [16]. In our limited experience, DCIS showed both microcalcifications in mammographies and *ductal enhancement* in CE-MRM.

As far as MR images analysis is concerned, many Authors have evaluated only the contrast enhancement of any formations, on the basis of acquired knowledge concerning the vascularization of the neoformations [18,19].

Other studies have indicated that quantitative analysis of the formations alone does not allow any certain distinction between malignant and benign formations as the radiographic contrast enhancement of the mammary gland is modified during the various phases of the menstrual cycle [13,21].

Subramanian et al. [1] have suggested that signal–intensity curve analysis provides a preliminary means to locate suspicious volumes within the breast, which can then be examined more carefully using additional metrics, such as location, shape and other morphological features.

Also in our study we did encounter some pitfalls in differentiating the nature of the mammary formations using quantitative analysis of the radiographic contrast enhancement as the main diagnostic parameter. In agreement with some literature [4,6], our study indicated the washout enhancement pattern as one of the parameters capable of defining the nature of the pathological formation (out of 220 lesions in 210 patients, 157 malignant lesions displayed this feature). Moreover, also the borders and the enhancement degree were important to give a final MRI diagnosis, as other authors have concluded [21–24].

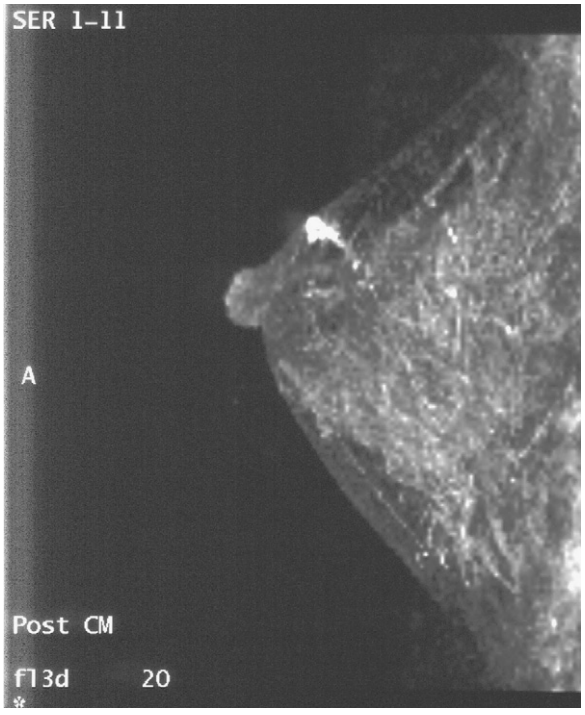

Fig. 3. Invasive ductal carcinoma in a 39-years-old woman. Not-palpable. Dynamic-contrast-enhancement-MRM (DCE-MRM), sagittal scan, MIP of early post-contrast phase. Linear ductal enhancement in the same area of microcalcifications at X-ray mammography (not shown). An evident washout was absent in the delayed phase of DCE-MRM (not shown).

In recent reports it has been confirmed that the validity of a trade-off between spatial and temporal resolution analysis [27].

The application of our diagnostic algorithm is based upon a morphological analysis associated with contrast kinetics evaluation of the mammary formations in DCE-MRM. In our study we have re-elaborated the diagnostic instrument previously suggested by others in a retrospective research [6]: we extended a prospective application to a larger number of cases. Furthermore, we based our analysis upon different parameters to diagnose the nature of the formation. Our study differs from the previous pilot report of Kinkel et al. [6] also in the method of selection of eligible patients: not only breasts with palpable or mammographic lesions, but also the controlateral negative breast was imaged in our work. A recent confirmation of the importance of bilateral examination has been furnished by other authors who have founded contralateral breast cancers in 9% (4/44) of the breast cancer patients [28].

This interpretative model, in our opinion, is capable not only to increase the method's specificity without reducing its sensitivity, but is also practical and easy to use.

Furthermore, we have evaluated in a consistent group of patients both breasts by only one contrast dose. Imaging of both breasts in sagittal planes offers potential efficiencies by not imaging the empty space between the breasts.

The visual assessment, in our experience, has represented a valid and intra-observer (Table 4) reproducible method to evaluate the morphologic and dynamic features of contrast enhancement of breast MRI diagnosed masses. We have tested the validity of visual assessment in a preliminary study on 100 patients.

Our results agree with those of using the same qualitative method [25,26,27].

Evaluations of MIP images has been the most important step in formulating our diagnostic impression. In our opinion, evaluation of MIP images, extracted from 3D subtraction series, is a rapid tool, that permits to assess probable malignant volumes. The hardware and the software actually in use in our Department (Avanto, Siemens, Erlangen, Germany) automatically provide subtraction and MIP images in DCE-MRM examinations, while in our work with the Magnetom Vision Plus we had to plan any series manually.

A progress in 3D evaluation of lesions in DCE-MRM has been showed by Subramanian et al. [1]. Their approach permits interactive manipulation of the signal–time curves, to rapidly assess probable malignant tumors.

Our effort to improve the morphological evaluation without lessening the kinetic parameter is similar in its results to the recent work of Kuhl et al. [27]: a standard dynamic protocol (256×256 matrix, 69 s per acquisition), similar to our MRM protocol was compared in a separate day with a modified dynamic protocol (400×512 matrix, 116 s per acquisition).

Table 5
Spatial resolution (voxel) in MRM. (Machine: Siemens 1.5 T Magnetom Vision Plus; TR, 5–15; TE, 3–5).

	FOV (mm)	Matrix	Slice thickness (mm)	Pixel (mm)	Voxel (mm^3)	TA (min:s)
a.	180 × 350	105 × 256	2	1.7 × 1.3	4.6	1:0
b.	320 × 320	252 × 256	1.5	1.2 × 1.2	2.4	2:59
c.	200 × 200	252 × 256	3	0.8 × 0.8	1.9	1:50
d.	125 × 200	192 × 512	1.5	0.5 × 0.4	0.2	2:59

Systematic qualitative analysis of morphologic features and region-of-interest-based analysis of enhancement kinetics were performed. Increased spatial resolution significantly improved diagnostic confidence and accuracy at dynamic MR imaging, even if this improvement occurred at the expense of temporal resolution. Loss of kinetic information regarding enhancement rates proved to be not diagnostically relevant because enhancement rates showed broad overlap between benign and malignant lesions and were therefore of only limited diagnostic use in the individual patient. Kinetic information regarding time course pattern was preserved and confirmed as having high specificity and high positive predictive value.

These results encourage our effort to increase spatial resolution, aimed to reduce unnecessary surgical procedures in benign processes of breast.

Our study has nevertheless several limitations or critical points: in examinations of the large breasts, was used an *acquisition time* longer than 87 s; *visual assessment* is operator-dependent and should be improved by computerized quantitative analysis; *misregistrations* has been limited only by physical tools, without processing the possible artifacts; some *benign lesions* did not receive histological confirmation; *postoperative MR imaging* has been not routinely performed to confirm lesion retrieval; some subgroups contained *few lesions*, therefore the conclusions about these features need further evaluations; and finally, when we have started our prospective analysis, *BI-RADS atlas* was in progress, and the terms assessed may not represent those in the finalized version.

Times of acquisition (TA) longer than 87 s in a consistent number of women with large breasts (16/150) were used in our trial. The available machine offered a choice of different techniques, to obtain a better temporal resolution or on the opposite side a better space resolution. In a previous trial in 100 women with 67 lesions, before the present prospective work, we utilized long TA (5′19″); an acquisition matrix of 256 × 256. The same protocol had been previously used by other authors [25]. One limitation of this protocol was the necessity to scan the controlateral breast in a deferred evaluation, with a second dose of contrast medium [4,5]. Another limitation was that with this long TA, late enhancement merged with early enhancement, at the expenses of the temporal resolution.

Also in the present series, without a deferred evaluation of the second breast, the main limitation in the examinations with an acquisition time longer than 90 s (110 s) was a systematic delay regarding wash-in and wash-out information from the second breast to be examined. For most breasts, we utilized a technique with a shorter time of acquisition (87 s, Table 5).

In all cases, voxels were less than 2.9 mm^3. The spatial resolution therefore was above the minimum used in a recent multitrial [36], but slightly less than the value (1.5 mm^3) that some state-of-the-art centers [5] have defined "high resolution" [5,36].

The new machine in our institution (Siemens, Avanto) offers a high-resolution protocol with an enough short acquisition time (91 s), that allows the imaging of both breasts in a sagittal sequence, without a significant delay in the second breast that is being examined.

Visual evaluation is obviously operator-dependent. Inter-agreement variability in our research (Table 4), in our opinion, can be linked more to a different experience between the readers in breast MR imaging.

Automated analysis has been proposed as a better option in clinical research, to provide objective assessments of contrast washin/washout characteristics across an entire image, several suggestions have been formulated, with different levels of difficulty and confidence in some recent works [29,30]. In an extensive trial, lesion rating (as benign, probably benign, indeterminate, suspicious, or highly suggestive of malignancy) and probability of malignancy calculated with computerized analysis were included as covariates in logistic regression analysis to obtain a combined model [29]. The performance of the model was compared with that of clinical reading alone and with of computerized analysis alone in a set of 72 clinically and mammographically occult lesions not used to train the computerized analysis system in 60 patients. Performance of reading in the clinical setting, as indicated by area under the ROC curve, was similar to that of computerized analysis. Significant overall improvement in performance was obtained with the combined model. Improvement was accomplished mostly in characterization of lesions rated indeterminate or suspicious by radiologists.

4.1. Misregistration

We have attained suppression of the fat signal by post-processing. Two advantages of image subtraction are minimized acquisition times, because inversion-recovery and spectral lipid-centered prepulse are not used, and insensitivity to field inhomogeneity [5].

The major disadvantages of image subtraction are decreased signal-to-noise ratio and sensitivity to patient motion, which can result in misregistration [5].

Female breast are scanned in a pendant position and therefore are amenable to non-linear deformation. Involuntary movement such as rolling of the patient, breathing, gravitation effects also cause motion [31]. The quality of subtraction images can be deteriorated by motion-related artifacts. These subtraction artifacts are expressed in extensive black-and-white stripes overlaying relevant structures [32]. Artifacts occur especially at the outer body contour and at high contrasting internal structures. In a maximum intensity projection (MIP) of 3D CT or MRI subtraction data, the artifacts of each individual slice are added together, sometimes resulting in an uninterpretable MIP image [32].

Beier et al. [32] proposed an image registration procedure *prior* to the digital subtraction allowing an enhanced visualization of the contrast agent. The object displacement was detected by analysis of image deformations in small local regions, based upon the leastsquare method for comparison of template similarity and the technique of elastic image warping. The algorithm worked fully automatically. The registration procedure provided good results in the suppression of subtraction artifacts and in the enhancement of vascular structures. Due to the extensive necessary calculations, the computation time was high: approximately 60 s for template comparisons and 10 s for image unwarping for one pair of slices. Thus, the calculation of a complete tomographic sequence may last for 1 or 2 h. Whereas no user interaction was required for this registration process, this task was usually performed off-line.

Nonrigid methods of registration has been proposed by other authors (mainly physicists) to reduce the problem of misregistrations [33–35]. The approach of Rueckert et al. [33], presented for the nonrigid registration of contrast-enhanced breast MRI, based upon a hierarchical transformation model of the motion of the breast.

One major problem with nonrigid image registration techniques was (until 2003) their high computational cost. Therefore, these methods have found limited application to clinical situations where fast execution is required, e.g., intraoperative imaging. When we began our present work, in 2001, a practical option to reduce misregistration effects without time-consuming procedures was not available. The problem of the time-consuming procedure has been significantly reduced by subsequent investigations (after 2003). Schnabel et al. [34] presented a parallel implementation of a nonrigid image registration algorithm. It was shown that its serial component is no more than 2% of the total computation time, allowing a speedup of at least a factor of 50. In most cases, the theoretical limit of the speedup is substantially higher (up to 132-fold in the application examples presented in their paper). Another work [35] has been based on the simulation of physically plausible, biomechanical tissue deformations using finite-element methods.

Although some artifacts due to the respiratory or cardiac movement were visible in subtraction images and in MIP images in 65/157 lesions of our patients, they did not impair in all cases the ability to visualize and analyze the regions of enhancement. Actually, 14 lesions in 12 patients in our present series of 220 lesions in 210 women (6,6%) were excluded from the evaluation, due to heavy motion artifacts. The last version of the double breast coil in our magnet (Avanto, Siemens, Erlangen, Germany) is equipped with lateral plates, to compress the breast and so to strongly limit motion and related artifacts. By the new equipment, we have experienced a more limited evidence of misregistration (about 1%).

References

[1] Subramanian KR, Brockway JP, Carruthers WB. Interactive detection and visualization of breast lesions from dynamic contrast enhanced MRI volumes. Comput Med Imaging Graph 2004;28:435–44.
[2] Helbich TH. Contrast-enhanced magnetic resonance imaging of the breast. Eur J Radiol 2000;34:208–19.
[3] Liberman L, Morris EA, Lee M, Kaplan JB, La Trenta LR, Menell JH, et al. Breast lesion detected on MR imaging: features and positive predictive value. AJR Am J Roentgenol 2002;179:171–8.
[4] Orel SG. MR imaging of the breast. MRI Clin North Am 2001;9:273–88.
[5] Orel SG, Schnall MD. MR imaging of the breast for the detection, diagnosis, and staging of breast cancer. Radiology 2001;220:13–30.
[6] Kinkel H, Helbich TH, Esserman LJ, Barclay J, Schwerin E, Sickles E, et al. Dynamic high-spatial resolution MR imaging of suspicious breast lesions: diagnostic criteria and interobserver variability. Am J Roentgenol 2000;175:35–43.
[7] Schnall MD, Ikeda DM, Lesion Diagnosis Working Group. J Magn Reson Imaging 1999;10:982–90.
[8] Kristoffersen WM, Aspelin P, Sylvan M, Bone B. Comparation of lesion size estimated by dynamic MR imaging, mammography and histopathology in breast neoplasm. Eur Radiol 2003;13:1207–12.
[9] Friedrich M. MRI of the breast: state of art. Eur Radiol 1998;10:707–25.
[10] Kaiser WA, Zeitler E. MR imaging of the breast: fast imaging sequences with and without Gd-DTPA. Radiology 1989;170:681–6.
[11] Nunes LW, Englander SA, Charafeddine R, Schnall MD. Optimal post-contrast timing of breast MR image acquisition for architectural feature analysis. J Magn Reson Imaging 2002;16:42–50.
[12] Matsubayashi R, Matsuo Y, Edakuni G, Satoh T, Tokunaga O, Kudo S. Breast masses with peripheral rim enhancement on dynamic contrast-enhanced MR images: correlation of MR findings with histologic features and expression of growth factors. Radiology 2000;217:841–8.
[13] Orel SG. MR imaging of the breast. Radiol Clin North Am 2000;38:899–913.
[14] Lorenzen J, Sinkus R, Adam G, Biesterfeldt M. Menstrual cycle dependence of breast parenchyma elasticity: estimation with magnetic resonance elastography of breast tissue during the menstrual cycle. Invest Radiol 2003;44:236–40.
[15] Nunes LW, Schnall MD, Englander SA, Charafeddine R. Optimal post-contrast timing of breast MR image acquisition for architectural feature analysis. J Magn Reson Imaging 2002;16:42–50.
[16] Gilles R, Zafrani B, Guinebretière JM, Meunier M, Lucidarme O, Tardivon AA, et al. Ductal carcinoma in situ: MR imaging-histopathologic correlation. Radiology 1995;196:415–9.
[17] Ikeda DM, Birdwell RL, Daniel BL. Potential role of Magnetic Resonance Imaging and other modalities in ductal carcinoma in situ detection. MRI Clin North Am 2001;9:345–56.
[18] Friedrich M. MRI of the breast: state of the art. Eur Radiol 1998;10:707–25.
[19] Mussurakis S, Buckley DL, Drew PJ, Fox JN. Dynamic MR imaging of the breast combined with analysis of contrast agent kinetics in the differentiation of primary breast tumors. Clin Radiol 1997;52:516–26.
[20] Nunes LW, Schnall MD, Orel SG, Hochman MG, Langlotz CP, Reynolds CA, et al. Breast MR imaging: interpretation model. Radiology 1997;202:833–41.
[21] Liu PF, Debatin JF, Caduff RF, Kacl G, Krestin GP. Improved diagnostic accuracy in dynamic contrast enhanced MRI of the breast by combined quantitative and qualitative analysis. Br J Radiol 1998;71:501–9.
[22] Nunes LW, Schnall MD, Orel SG. Update of breast MR imaging architectural interpretation model. Radiology 2001;219:484–94.
[23] Heywang-Köbrunner SH, Bick U, Bradley Jr WG, Boné B, Casselman J, Coulthard A, et al. International investigation of breast MRI: results of a multicentre study [11 sites] concerning diagnostic parameters for contrast-enhanced MRI based on 519 histopathologically correlated lesions. Eur Radiol 2001;11:531–46.
[24] Szabo BK, Aspellin P, Bone B, Kristoffersen M. Dynamic MR Imaging of the breast: analysis of kinetic and morphologic diagnostic criteria. Acta Radiol 2003;44:379–86.
[25] Kuhl CK, Mielcareck P, Klaschik S, Leutner C, Wardelmann E, Gieseke J, et al. Dynamic breast MR imaging: are signal intensity time course data useful for differential diagnosis of enhancing lesions? Radiology 1999;211:101–10.
[26] Choi BG, Kim HH, Kim EN, Kim BS, Han JY, Yoo SS, et al. New subtraction algorithms for evaluation of lesions on dynamic contrast-enhanced MR mammography. Eur Radiol 2002;12:3018–22.
[27] Kuhl CK, Schild HH, Morakkabati N. Dynamic bilateral contrast-enhanced MR imaging of the breast: trade-off between spatial and temporal resolution. Radiology 2005;236:789–800.
[28] Wiener JI, Schilling KJ, Adami C, Obuchowski NA. Assessment of suspected breast cancer by MRI: a prospective clinical trial using a combined kinetic and morphologic analysis. AJR Am J Roentgenol 2005;184(3):878–86.
[29] Buckley DL, Kerslake RW, Blackband SJ, Horsman A. Quantitative analysis of GD-DTPA enhanced dynamic MR images by simplex minimization. Mag Resonan Mater Phys Biol Med.
[30] Deurloo EE, Muller SH, Peterse JL, Besnard APE, Gilhuijs KGA. Clinically and mammographically occult breast lesions on MR images: potential effect of computerized assessment on clinical reading. Radiology 2005;234:693–701.
[31] (a) Knopp MV, Weiss E, Sinn HP, Mattern J, Junkermann H, Radele J, et al. Pathophysiologic basis of contrast enhancement in breast tumors. J Magn Resonan Imaging 1999;10:260–6;
(b) Schnall MD, Ikeda DM, Lesion Diagnosis Working Group. J Magn Reson Imaging 1999;10:982–90.
[32] Beier J, Oellinger H, Richter CS, Fleck E, Felix R. Registered image subtraction for CT, MR and coronary angiography. Eur Radiol 1997;7:82–9.
[33] Rueckert D, Sonoda LI, Hayes C, Hill DL, Leach MO, Hawkes DJ. Nonrigid registration using free-form deformations: application to breast MR images. IEEE Trans Med Imaging 1999;8:712–21.
[34] Schnabel JA, Tanner C, Castellano-Smith AD, Degenhard A, Leach MO, Hose DR, et al. Validation of nonrigid image registration using finite-element methods: application to breast MR images. IEEE Trans Med Imaging 2003;2:238–47.
[35] Rohlfing T, Maurer Jr CR. Nonrigid image registration in shared-memory multiprocessor environments with application to brains, breasts, and bees. IEEE Trans Inf Technol Biomed 2003;1:16–25.
[36] Schnall MD, Blume J, Bluemke DA, DeAngelis GA, DeBruhl N, Harms S, et al. Diagnostic architectural and dynamic features at breast MR imaging: multicenter study. Radiology 2006;238(1):42–53.

Giuseppe Potente was born in Cosenza, Italy, in 1950. He received a degree from the University of "La Sapienza", Rome, Italy, in 1974 and a specialty in Radiology, from the same University, in 1985. Since 1975, he has been with the same University where he is Associate Professor in Radiology from 1988. His research interests focus on lung diseases, lymphomas, breast diseases, and early diagnostic of neoplasms.

Daniela Messineo was born in Rome, Italy in 1962. She received Degree of Medical School Medicine and Surgery in 1988 from University of Rome "La Sapienza" and specialty in Radiology School of Medicine and Surgery in 1994 from University of Rome "La Sapienza". At present she works as a Researcher at Radiological Sciences Department in Complex Unity of ENT, she still work in Uroradiology and Dental Radiology.

Sara Savelli was borne in Rome, Italy, in 1979. She received a degree from the University of "La Sapienza", Rome, Italy, in 2004. She is resident in the same University.

Claudia Maggi was borne in Rome, Italy, in 1977. She received a degree from the University of "La Sapienza", Rome, Italy, in 2003. She is resident in the same University.